Use of Radiation Detection, Measuring, and Imaging Instruments to Assess Internal Contamination from Intakes of Radionuclides

Part VI: Field Tests and Feasibility Studies of PET Scanners

Prepared by

T. G. Turkington, R. Anigstein, and J. C. Engdahl

S. Cohen & Associates
1608 Spring Hill Road
Vienna, Virginia 2218

Contents

Tables

Figures

PREFACE

Part I of the present series described a study to evaluate radiation detection and imaging systems commonly found in hospitals to determine their suitability for rapidly scanning individuals for internal contamination, and to develop recommendations regarding their potential use (Anigstein et al. 2007a). That report described the measurement of count rates from single discrete radioactive sources of ^{60}Co, ^{137}Cs, ^{192}Ir, and ^{241}Am, using a Philips AXIS gamma camera, an Atomlab thyroid uptake system, and a Ludlum waste monitor.

Part II extended the earlier investigation by using realistic anthropomorphic phantoms to study the responses of four instruments to five radionuclides distributed in the lungs (Anigstein et al. 2007b). The experimental measurements were performed on sources in the lung region of a Rando Phantom—an anthropomorphic phantom that contains a human skeleton embedded in a tissue-equivalent urethane rubber. Count rates from each of five radionuclides—^{60}Co, ^{90}Sr, ^{137}Cs, ^{192}Ir, and ^{241}Am—were measured on the Siemens e.cam Fixed 180 gamma camera, an Atomlab thyroid probe, a Ludlum survey meter, and a Ludlum waste monitor. The Los Alamos MCNPX (Monte Carlo N Particle eXtended) computer code was used to calculate calibration factors that relate count rates on these instruments to lung burdens of each of the five nuclides. A mathematical model of each of the instruments was constructed, using engineering drawings and other data obtained from the manufacturers. This model was combined with an MCNP model of a Rando Phantom, constructed from CT scans of this phantom (Wang et al. 2004). The combined model was used to simulate the response of each instrument to sources in the phantom. The agreement between the calculated and measured responses validated the MCNP models of the four instruments.

Part III (Anigstein et al. 2007c) extended the investigations to the Philips SKYLight camera. The study was narrowed to three of the five radionuclides reported in Part II: ^{60}Co, ^{137}Cs, and ^{241}Am. This study encompassed measurements and corresponding MCNP simulations of sources of the three nuclides located in the lung region of a Rando Phantom. In addition, measurements and corresponding simulations were carried out with the source capsules in air. The agreement between the calculated and measured responses validated the MCNP model of this instrument.

Part IV (Anigstein et al. 2010) extended the earlier investigations to the response of the Philips SKYLight camera to bremsstrahlung x rays following the β decay of ^{90}Sr and its short-lived daughter, ^{90}Y. As reported in part II, the count rates recorded by the Siemens e.cam gamma camera exposed to ^{90}Sr sources in the Rando Phantom were approximately 50% higher than the values calculated with the MCNP model. Preliminary studies of count rates recorded by the Philips SKYLight camera exposed to ^{90}Sr sources in air also showed significant discrepancies with the corresponding MCNP calculations. Further measurements and Monte Carlo simulations of ^{90}Sr were therefore undertaken in an attempt to resolve this problem. These studies utilized, as a primary standard, a calibrated source of ^{90}Sr procured from the National Institute of Standards and Technology. Measurements and Monte Carlo simulations of this source, which was in the form of an aqueous solution sealed in a glass ampoule, were supplemented by further studies on the encapsulated sources described in part II. The agreement between the calculated

and measured responses was adequate to justify the use of the model for simulating the response of this camera to distributions of ^{90}Sr/^{90}Y in the human body.

Part V (Anigstein and Olsher 2010) developed calibration factors to enable the use of gamma cameras for assessing intakes of radionuclides and the resulting doses. The study utilized biokinetic models to determine the retention of activity taken into the body and the distribution of such activity among different regions of the body as a function of time following exposure. Normalized count rates from activities of six radionuclides—^{60}Co, ^{90}Sr, ^{131}I, ^{137}Cs, ^{192}Ir, and ^{241}Am—in various anatomical regions of children of five ages and adult men and women were calculated by MCNPX. Adult men and women were represented by the NORMAN and NAOMI voxel phantoms (Dimbylow 1998, 2005), while children were represented by the revised ORNL phantom series described by Han et al. (2006). The Siemens e.cam and Philips SKYLight gamma cameras were represented by models developed during the studies described in parts II and III, respectively.

The present study attempts to determine if it is feasible to use PET scanners to assess intakes of inhaled radionuclides by exposed individuals, in a manner similar to gamma cameras. The study was motivated by the large number of PET scanners installed in the United States, and the fact that these instruments, in common with gamma cameras, have radiation detectors with large areas and volumes that, in principle, would be sensitive to relatively low levels of photon radiation. However, unlike gamma cameras, which can be set to detect and count photon over a wide energy range, PET scanners are primarily designed to detect positron annihilation radiation, which has an energy of 511 keV. One aim of the investigation is to determine the ability of the various models of PET scanners to detect nuclides that emit lower-energy radiation.

The present report was revised to reflect the new series title and part number, to update this preface, and to incorporate a revised list of references. The remainder of the text is unchanged.

Chapter 1

RADIATION MEASUREMENTS

A radiological emergency, such as the detonation of a radioactive dispersion device (RDD or "dirty bomb"), could lead to the inhalation of airborne radioactive material by a large number of people. There would be a need to rapidly assess this inhaled activity and determine the need for medical intervention.

Studies presented in Parts I, II, and III of the present series of reports demonstrated that radiation detection and imaging systems commonly found in hospitals, including gamma cameras used in nuclear medicine, can be used to screen exposed individuals for radioactive materials inside the body. The current study extends the earlier investigation by determining the feasibility of using PET scanners for this purpose. The present chapter describes a series of measurements to evaluate the detection efficiency of a commercial whole-body PET scanner for radionuclides emitting a wide range of photon energies.

1.1 Introduction

PET and PET/CT scanners have become much more widespread in United States in the last 10 years, from fewer than 100 to more than 1,000. PET scanners are designed to detect the 511 keV photon pairs from positron annihilation, in coincidence. The fundamental measurement on a PET scanner is therefore the number of coincidence events on each detector pair. However, the number of "single" events may also be recorded, where a single event is any photon detection regardless of coincidence with another detector. Singles count rates are always much higher than coincidence rates.

1.2 Materials and Equipment

1.2.1 PET Scanner

The study was performed on a Discovery STE PET/CT system made by GE Healthcare Technologies, that is located in the Duke University Medical Center PET Facility. A view of the front (CT) end of the scanner is shown in Figure 1, while the PET end of the scanner is shown in Figure 2. The scanner contains 13,440 bismuth germanate (BGO) detectors arranged in 280 blocks. Each detector is a BGO crystal measuring $5 \times 6 \times 30$ mm. Each block consists of 48 detectors in a 6×8 array; the blocks form four rings. The system has an energy resolution of approximately 17% at 511 keV, averaged over all detectors. The scanner has two main modes of operation, which are illustrated in Figure 3. In 2D mode, tungsten septa are placed in front of the crystal seams, preventing the detection of photons not emitted within the transaxial plane. In 3D mode, the septa are retracted, and all coincidences are recorded, regardless of the rings in which the two photons are detected. For PET imaging, 2D mode greatly reduces background events and accidental coincidences, whereas 3D mode provides much higher sensitivity (detected true counts per injected dose).

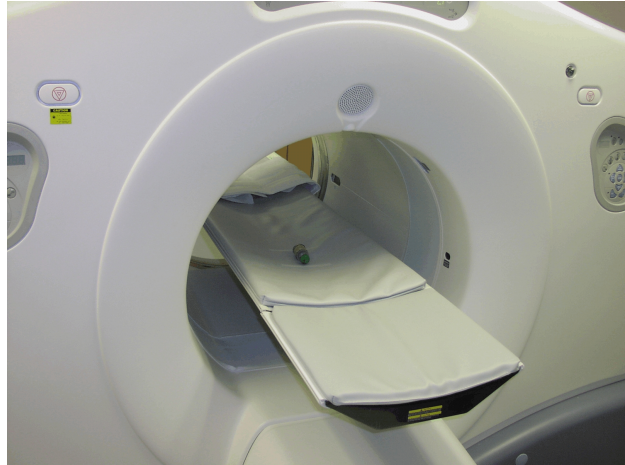Figure 1. Discovery STE PET/CT scanner: front view

Figure 2. Discovery STE PET/CT scanner: view from PET end, showing source on table

For the present study, data were acquired in both modes. Even for single photon emission, it was assumed that 3D mode would allow higher sensitivity, but would also register higher background counts. The 2D mode could, in principle, provide a detailed axial profile of the radionuclide distribution in a patient.

1.2.2 Radioactive Sources

The experiment utilized sources of five radionuclides with known activities—^{57}Co, ^{60}Co, ^{99m}Tc, ^{125}I, and ^{137}Cs—that were readily available in the Radiology Department of the Duke University Medical Center. Each ^{57}Co, ^{60}Co, and ^{137}Cs source was dispersed in a solid epoxy resin inside in a 20 mL bottle. Iodine-125 was essentially a point source inside a small, shallow cavity in a 2-cm diameter lead disc. The

Figure 3. Schematic Illustration of 2D and 3D PET Scanner Modes

aperture of this cavity subtended a solid angle of approximately $\frac{4}{3}\pi$ steradians. The ^{99m}Tc source consisted of 1 mL of solution in a 3-mL syringe. These nuclides emit x and γ rays with energies of 27 to 1,333 keV, thus spanning the energy range of γ-emitting radionuclides likely to be used in an RDD. More detailed information on these sources is presented in Table 1.

1.3 Experimental Measurements

The normal lower and upper level discriminator (LLD and ULD) settings for this system are 375 keV and 650 keV for 2D imaging, and 425 keV and 650 keV for 3D, respectively. For this
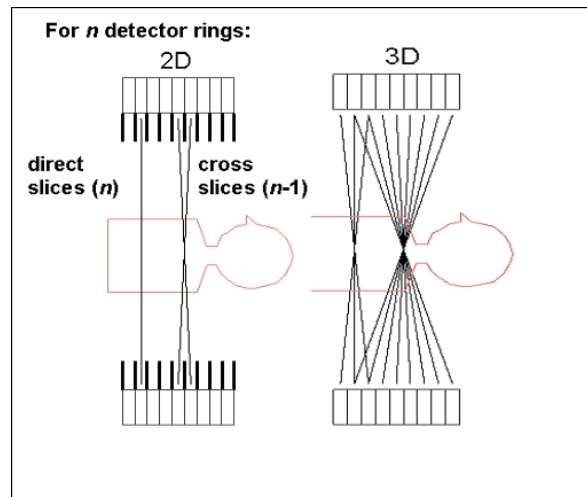
study, measurements were made with LLD set at 10 keV and ULD at 800 keV. It should be noted that this LLD setting is most likely not the only low-energy threshold in effect: front-end electronics are likely to remove signals significantly higher than 10 keV.

Table 1. Radioactive Sources Used in Study

Nuclide	Activity (MBq)	Physical form[a]	Principal photon spectra		
				E (keV)	I (%)
				27.20	40.6
				27.47	75.7
				30.94	6.83
				31.00	13.2
I-125	43.73	lead disc		31.24	0.12
				31.70	3.81
				31.77	0.58
				35.49	6.68
			$<E>$	28.37	I_{tot} 147.52
				122.06	85.6
Co-57	143.23	epoxy		136.47	10.68
			$<E>$	123.66	I_{tot} 96.28
Tc-99m	33.23	syringe		140.51	89
Cs-137	4.88	epoxy		661.66	85.1
				1173.24	99.97
Co-60	1.721	epoxy		1332.5	99.99
			$<E>$	1252.87	I_{tot} 199.96
Am-241	~0.037	smoke detector		59.5412	35.9

[a] See Section 1.2.2

All measurements of count rates from radioactive sources and background were performed in both 2D and 3D modes, using a counting time of 1 minute. Each acquisition resulted in a raw data file, which included the counts per crystal and the counts per crystal pair. The counts and crystal data were extracted from each raw data file. Counts were summed over all crystals, resulting in a single count being measured for each scan.

1.3.1 Background Count Rates

An initial set of background count rates was measured using the normal LLD and ULD settings cited in the previous section in order to observe the effect on the background rate of the wider energy window used in the experiment. Background counts in the energy window used for this study were measured before and after each set of source measurements. These background counts are listed in Table 2. The wider energy window results in more than a 4-fold increase in the count rates in both 2D and 3D modes. For the experimental measurements, the background was quite constant over the 100-minute period of the measurements. As shown in Table 2, the

standard deviations (σ_D) of the six 2D and 3D counts are not much greater than would be predicted on the basis of Poisson statistics alone.

1.3.2 Experimental Count Rates

Count rates were measured with each of the five sources on the scanning table. Count rates from the ^{60}Co source were also measured with the source on a table approximately 2 m from the scanner. This was done to study the effects of nearby activity on measured counts, especially from the highly penetrating photons from this nuclide. The results of the measurements are listed in Table 3. The nuclides are listed in the order in which the measurements were performed to facilitate comparison with the corresponding background rates listed in Table 2.

Table 2. Background Count Rates

Description	Energy window (keV)		Sequence	Mode	Raw counts (1 min)	Count rate (cps)
	LLD	ULD				
Normal settings	375	650	Initial	2D	222,655	3,711
	435			3D	545,095	9,085
Experimental	10	800	1	2D	912,631	15,211
				3D	2,273,051	37,884
			2	2D	912,501	15,208
				3D	2,274,846	37,914
			3	2D	911,053	15,184
				3D	2,275,753	37,929
			4	2D	914,318	15,239
				3D	2,275,847	37,931
			5	2D	914,106	15,235
				3D	2,277,877	37,965
			6	2D	915,073	15,251
				3D	2,280,697	38,012
			Mean	2D	913,280	15,221
				3D	2,276,345	37,939
			σ_D	2D	1,481	25
				3D	2,645	44

In all cases, a measurable signal was obtained that was significant compared to background variations during the time of the measurement. It should be noted that the experiment was performed on a Saturday, when no radioactive patients were present and any PET radionuclides used during the week would have decayed. Clearly, the ability to detect small signals would deteriorate in the presence of a high or varying background. The ratios of the normalized count rates in the 3D to 2D modes are greatest for the lowest energies, as expected, since the tungsten septa have decreasing effect on higher-energy photons.

For all nuclides except ^{60}Co, the counts per photon increase with increasing photon energies, indicating that the counting efficiency increases with energy. The efficiency for ^{60}Co is slightly less than for ^{137}Cs in 2D mode and significantly less in 3D. This is most likely because the photopeaks from the two principal [60]Co γ rays lie above the 800 keV ULD.

As discussed in Section 2.1, the system is not capable of counting the 27–35 keV photons emitted by [125]I. The measured count rates from this nuclide are due to pulse pileup: multiple photons are incident on a single block of detectors during a time period too short for the individual photon energies to be resolved. Using a simplified geometry and assuming complete energy deposition by each incident photon, we calculated that, for an assumed integration time of 1 μs, a count rate of approximately 100 kcpm would be registered by the system in 3D mode from three photons being incident on each detector during this integration time. The average total energy registered for each triple coincidence event would be ~85 keV. The count rate from double coincidences for the same assumed integration time would be ~5 Mcpm. Since the background-corrected count rate in 3D mode is ~100 kcpm, we conclude that the count rate is due to triple coincidences, and that the system is incapable of registering photons with energies below about 57 keV, which is twice the average energy of the principal photons emitted by this nuclide.

Table 3. Results of Experimental Measurements

Nuclide	$<E>$[a] (keV)	Mode	Counts			
			Raw[b]	Net[b,c]	Per photon	cps/Bq
Co-57	123.66	2D	1.97e+08	1.96e+08	2.37e-02	2.28e-02
		3D	7.84e+08	7.82e+08	9.45e-02	9.10e-02
Co-60	1,252.87	2D	1.74e+07	1.65e+07	7.99e-02	1.60e-01
		3D	2.63e+07	2.40e+07	1.16e-01	2.33e-01
		2D[c]	1.21e+06	2.97e+05	1.44e-03	2.88e-03
		3D[c]	2.67e+06	3.97e+05	1.92e-03	3.84e-03
Cs-137	661.66	2D	2.27e+07	2.18e+07	8.74e-02	7.43e-02
		3D	4.44e+07	4.21e+07	1.69e-01	1.44e-01
I-125[e]	28.37[f]	2D	9.35e+05	2.07e+04	5.34e-06	7.88e-06
		3D	2.38e+06	1.02e+05	2.64e-05	3.89e-05
Tc-99m	140.51	2D	5.32e+07	5.23e+07	2.95e-02	2.62e-02
		3D	2.13e+08	2.11e+08	1.19e-01	1.06e-01

[a] Average energy of photons in measurable range (see Table 1)

[b] Counting time = 1 min

[c] Corrected for background—average of background counts before and after experimental measurements

[d] Source on table 2 m from scanner

[e] Source two thirds surrounded by lead shielding

[f] Average energy of all photons > 5 keV

1.4 Experimental Measurements on [241]Am

Americium-241 is one of the 10 radionuclides cited by the DOE/NRC Interagency Working Group on Radiological Dispersion Devices as being among the "isotopes of greatest concern" (DOE/NRC 2003, Appendix F). The results of the studies described in Section 1.3 do not clearly indicate whether this nuclide, with a principal γ ray of 59.5 keV, is detectable by this system. We therefore performed a simple experiment, using a commercial smoke detector which contains an [241]Am source. A legend on the detector indicated that the activity was < 1 μCi (37 kBq), while an article on the EPA Web site states: The average activity in a smoke detector source is about one microcurie . . . . (EPA 2007).

The results of the experiment are shown in Table 4. The net counts for the [241]Am source in the smoke detector are comparable to the differences in the background before and after the experimental measurement. A calculation based on a simplified geometry shows that the total count rate in 3D mode would be about 90 kcpm if the activity were 1 μCi, if all the 59.5 keV photons incident on the detectors were counted, and if there were no significant shielding of the source inside the smoke detector. It is clear that, were the system capable of detecting photons of this energy, a measurable count rate would have been registered, even if the activity were a fraction of 1 μCi.

Table 4. Experimental Measurements on [241]Am Source in a Smoke Detector

Description	Mode	Counts	Net counts
Initial background	2D	920,377	
	3D	2,294,655	
Am-241	2D	917,155	-2,451
	3D	2,293,333	251
Final background	2D	918,834	
	3D	2,291,510	

Chapter 2

ADDITIONAL INFORMATION AND CONCLUSIONS

Additional information on PET scanners from the three major U.S. suppliers was obtained from published sources, corporate Web sites, and industry experts.

2.1 GE Healthcare

Figure 4 shows energy spectra of a positron-emitting source measured on a GE Healthcare PET scanner. The peak energy of 511 keV corresponds to Channel 160 on these graphs. There appears to be a sharp drop in counts at about Channel 25, which corresponds to about 80 keV, assuming a linear scale that extends to zero. These graphs confirm the results of the experiment on the ^{241}Am in a smoke detector, described in Section 1.4. We conclude that ^{241}Am is not detectable by this system.

Figure 4. Energy Spectra of GE PET Scanner

2.2 Siemens Medical Solutions USA

The PET scanners currently distributed by Siemens Medical Solutions USA contain detectors made of lutetium oxyorthosilicate (LSO), which has the chemical formula Lu_2SiO_5. The radioactive isotope ^{176}Lu constitutes 2.59% of natural lutetium. As a result, LSO has a specific activity of about 39 Bq/g. Lutetium-176 is a β-γ emitter: the principal β ray has an end-point energy of 596 keV, while the principal γ rays have energies of 202 and 307 keV. The β and γ rays can trigger counts in the crystals in which they are emitted; the γ's could also give rise to counts in other crystals in the scanner. Yammato et al. (2005) measured the background singles rate in the Siemens ACCEL LSO-based PET scanner for different settings of the low-energy threshold. The rates increased as the threshold was decreased, the highest rate, ~2.4 Mcps, corresponding to about 150 keV, the lowest threshold used in the study. (A rate of 2.4 Mcps is equal to 1.44×10^8 counts in one minute.)

Given the objective of the present study—the suitability of PET scanners to assess inhaled activity in exposed individuals—it is instructive to estimate the effect of the background rate on the minimum detectable activity (MDA) of such an LSO-based system. The MARSSIM manual (NRC 2000) presents an analysis of the minimum activity that can be detected by a radiation measuring instrument. Based on that discussion, we derived the following equation to calculate the MDA:
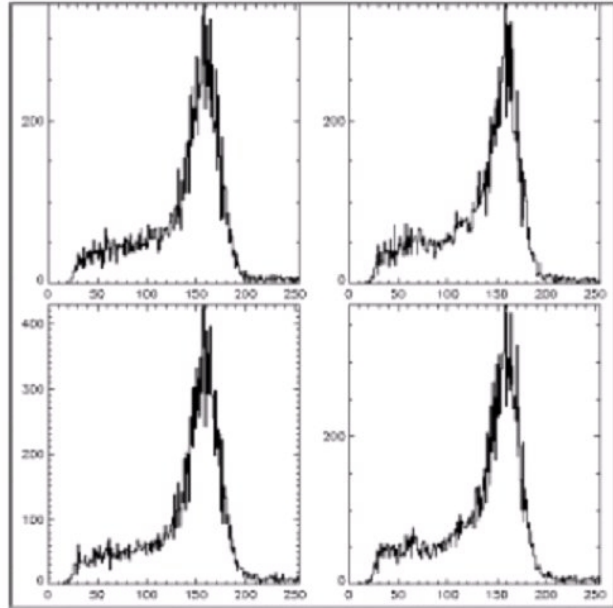
$$A_i = \frac{3 + 4.65\sqrt{bt_c}}{n_i t_c}$$

A_i = minimum activity of radionuclide i (Bq)

b = background count rate of detector (cps)

t_c = counting time for both background and suspected radioactive source (s)

n_i = normalized count rate of detector exposed to radionuclide i (cps/Bq)

We use the measured count rate of ^{137}Cs in the GE Healthcare PET scanner in 3D mode as a surrogate for the sensitivity of the LSO-based system.[1] As shown in Table 3, the normalized rate for this nuclide is 0.144 cps/Bq. Inserting this value into the above equation, and assuming a counting time of 1 minute, we obtain an MDA of ~6,460 Bq. This value, which is for a point source at the center of the scanner's field of view and is thus an optimum value, can be compared to the MDA for ^{137}Cs uniformly distributed in the lungs of an anthropomorphic phantom, measured with the Siemens e.cam gamma camera. The latter value, which is derived from a Monte Carlo simulation, was calculated to be 127 Bq for a 1-minute count (Anigstein et al. 2007b). The value would be lower for a point source at the center of the field of view of the camera. Thus, an LSO-based PET scanner is much less sensitive than a gamma camera, even to radionuclides with energies that fall into the energy window of the scanner.

2.3 Philips Medical Systems N.A.

Philips Medical Systems, N. A., distributes several models of PET and PET/CT scanners. The basic model is the Allegro, which uses detectors made of gadolinium orthosilicate (GSO) (Smith 2007). The latest model is the Gemini TF PET/CT—the PET subsystem uses detectors made of cerium-doped lutetium yttrium oxyorthosilicate (LYSO), a mixture of approximately 90% Lu_2SiO_5 and 10% Y_2SiO_5. Similar to the Siemens scanners, these detectors contain ^{176}Lu (albeit in a slightly lower concentration), and are therefore subject to a similar limitation in detecting low levels of internal activities due to a high background count rate.

The Philips PET scanners have preset energy windows. The normal windows are relatively narrow and are centered on 511 keV. The energy range of the Allegro scanner could, in principle, be adjusted to detect events as low as 200 keV. However, changing the energy windows on Philips PET scanners normally requires the intervention of a Philips field service engineer. These settings can be modified by a user only under a research agreement with Philips. Thus, unless prior arrangements were made with Philips, these scanners could be used to detect radionuclides only by counting events that fall within the preset energy window.

---

[1] The actual sensitivity of the Siemens PET scanner will be about 30% less because Z_{eff} = 65 for LSO vs 75 for GSO. Furthermore, the Siemens detectors are 2 cm thick vs 3 cm for the GE.

2.4 Conclusions

The PET scanners currently in use in the United States have low-energy cutoffs that would preclude their use in detecting ^{241}Am or any other nuclides with principal photon emissions below 80 – 250 keV, depending on the model. Furthermore, the background count rates in singles mode, even of scanners that do not use detectors containing lutetium, are much higher than those of gamma cameras. For example, the highest background count rate measured on the Siemens e.cam camera, with collimators removed and an energy window set to maximum width, was 867 cps (Anigstein et al. 2007b, Table 1-3). This can be compared to the average background of 15,221 cps in 2D mode and 37,939 cps in 3D registered on the GE PET scanner, as listed in Table 2. Measurements on both instruments were made in nuclear medicine facilities on a weekend, with no patients or other radioactive sources in the area. Based on these data, the minimum activities detectable by PET scanners are significantly higher than those detectable by gamma cameras.

On the other hand, the PET scanners offer an inherent advantage over gamma cameras in measuring high levels of activity of high-energy γ emitters such as ^{60}Co, ^{137}Cs, and ^{192}Ir. Because gamma cameras are limited to count rates of 300–500 kcps per detector, activities of these nuclides greater than 1–5 MBq, depending on the nuclide and the camera model, may not be assessed accurately due to dead-time counting losses. In a PET system, however, each detector block processes counts independently. If we assume the integration time to be 1 μs (a conservatively high assumption), then each detector could register 200 kcps with a 20% dead-time loss. The Discovery STE PET/CT system described in Section 1.2.1, with 280 detector blocks, could thus register a rate of 56 Mcps with reasonable accuracy. Based on the experimental results listed in Table 3, this would correspond to a point source of ~400 MBq (~11 mCi) of ^{137}Cs in 3D mode and twice that in 2D mode, which is two orders of magnitude greater than the maximum activity that could be accurately counted with a gamma camera.

REFERENCES

Anigstein, R., et al. 2007a. "Use of Radiation Detection, Measuring, and Imaging Instruments to Assess Internal Contamination from Intakes of Radionuclides. Part I: Feasibility Studies." http://www.bt.cdc.gov/radiation/clinicians/evaluation/pdf/Part_I.pdf

Anigstein, R., R. H. Olsher, and J. C. Engdahl. 2007b. "Use of Radiation Detection, Measuring, and Imaging Instruments to Assess Internal Contamination from Intakes of Radionuclides. Part II: Field Tests and Monte Carlo Simulations Using Anthropomorphic Phantoms." http://www.bt.cdc.gov/radiation/clinicians/evaluation/pdf/Part_II.pdf

Anigstein, R., et al. 2007c. "Use of Radiation Detection, Measuring, and Imaging Instruments to Assess Internal Contamination from Intakes of Radionuclides. Part III: Field Tests and Monte Carlo Simulations of Philips SKYLight Gamma Camera." http://www.bt.cdc.gov/radiation/clinicians/evaluation/pdf/Part_III.pdf

Anigstein, R., R. H. Olsher, and M. C. Erdman. 2010. "Use of Radiation Detection, Measuring, and Imaging Instruments to Assess Internal Contamination from Intakes of Radionuclides. Part IV: Response of Philips SKYLight Gamma Camera to ^{90}Sr." http://www.bt.cdc.gov/radiation/clinicians/evaluation/pdf/Part_IV.pdf

Anigstein, R., and R. H. Olsher. 2010. "Use of Radiation Detection, Measuring, and Imaging Instruments to Assess Internal Contamination from Intakes of Radionuclides. Part V: Calibration Factors for Gamma Cameras." http://www.bt.cdc.gov/radiation/clinicians/evaluation/pdf/Part_V.pdf

The DOE/NRC Interagency Working Group on Radiological Dispersal Devices (DOE/NRC). 2003. "Radiological Dispersal Devices: An Initial Study to Identify Radioactive Materials of Greatest Concern and Approaches to Their Tracking, Tagging, and Disposition." www.ssa.doe.gov/sp70/documents/RDDRPTF14MAY03.pdf.

Dimbylow, P. J. 1998. "Induced Current Densities from Low-frequency Magnetic Fields in a 2 mm Resolution, Anatomically Realistic Model of the Body." *Physics in Medicine and Biology 43*, 221–230.

Dimbylow, P. J. 2005. "Development of the Female Voxel Phantom, NAOMI, and its Application to Calculations of Induced Current Densities and Electric Fields from Applied Low Frequency Magnetic and Electric Fields." *Physics in Medicine and Biology, 50*, 1047–1070.

Environmental Protection Agency (U.S.) (EPA). 2007. "Smoke Detectors & Radiation." http://www.epa.gov/radiation/sources/smoke_alarm.htm.

Han, E., W. E. Bolch, and K. F. Eckerman. 2006. "Revisions to the ORNL Series of Adult and Pediatric Computational Phantoms for Use with the MIRD Schema." *Health Physics, 90*(4), 337-356.

Nuclear Regulatory Commission (U.S.) (NRC). 2000. "Multi-Agency Radiation Survey and Site Investigation Manual (MARSSIM)," NUREG-1575, Rev. 1. Washington, DC: Author.

Smith, S. F. (Senior Manager, PET Product Marketing, Philips Nuclear Medicine). 2007. <scott.smith@philips.com> "Re: PET Scanner " August 21, 2007, personal e-mail to Robert Anigstein, SC&A, Inc.

Wang, B., X. G. Xu, and C. H. Kim. 2004. "A Monte Carlo CT Model of the Rando Phantom." *American Nuclear Society Transactions*, *90*, 473-474.

Yamamoto, S. et al. 2005. "Investigation of Single, Random, and True Counts from Natural Radioactivity in LSO-based Clinical PET." *Annals of Nuclear Medicine 19*(2), 109–114. http://www.jsnm.org/files/paper/anm/ams192/ANM19-2-07.pdf.